Development of a Preliminary SST Planform Design Tool Using a Numerical Optimization Routine

Shin Matsumura*, John P. Sullivan+
Purdue University
West Lafayette, IN 47906 USA

Yuichi Shimbo⊥
National Aerospace Laboratory
Osawa, Mitaka, Tokyo 181-0015 Japan

ABSTRACT

A preliminary SST wing planform design program was developed using the simplex downhill method for numerical optimization and lifting surface theory for aerodynamic analysis. The wing planform was restricted to an arrow wing with a constant planform area, and the geometry was represented by at most seven independent design variables. The objective function of the optimization was the inviscid drag at design condition (M=2, C_L=0.1) with penalty functions for the violation of geometry constraints. Because the program only performs aerodynamic analysis, variables were bound or held constant based on multidisciplinary considerations such as structural and manufacturing restrictions, in order to avoid unrealistic planforms.

The results showed the design variables could be grouped into a set of primary variables (aspect ratio, slenderness ratio, sweep angle of inner leading edge) which played key roles to the optimization, and a set of secondary variables, primarily used to satisfy the geometry constraints. Finally, as a preparation for the multi-point design, the optimization was performed at several design Mach numbers and corresponding design lift coefficients while keeping the flight altitude and the weight of the aircraft the same. The resulting optimum geometry changed to trade off the induced drag from the high aspect ratio with the wave drag from the high leading edge sweep.

INTRODUCTION

To prepare for commercial flight in the 21st century, National Aerospace Laboratory (NAL) of Japan is promoting a high-priority research program for the next-generation supersonic transport (SST). The objective of the program is to develop design techniques/methods that will make the next-generation SST a reality.

One of the mandatory requirements for a SST is a low drag, high efficiency wing. Today, with massively paralleled supercomputers and workstations such as the ones present at NAL, the aerodynamic design of an aircraft and/or aircraft component is possible through the use of computational fluid dynamics (CFD). Different techniques are used at different design process stages, so that computing time is efficiently used. During the preliminary design stage, a large number of iterations are done with lower level analysis methods, to find a good starting point for detailed design. For such purposes, simple methods such as linear theory are very well suited.

Codes that use Carlson's Method for aerodynamic analysis, and the design of load distributions were developed at NAL by K. Yoshida, in [1]. By using these programs, an optimization program PLANFOPT for the wing planform design was developed. The purpose of this program was to find a starting point for a CFD-based detailed design.

---

* Student, School of Aeronautics and Astronautics
+ Professor, School of Aeronautics and Astronautics
⊥ Senior Researcher, Advanced Technology Aircraft Project Center

This paper will discuss the results shown by PLANFOPT in the design of a supersonic wing planform.

OPTIMIZATION ROUTINE

As with any optimization program, an iteration routine is necessary. This work implemented the simplex downhill method from [2]. The simplex method was chosen due to the simplicity of the algorithm, and because it uses only the values of the function evaluated and not the derivatives for the iteration. This makes the method inefficient in terms of the number of function evaluations it must perform, but it offers the advantage that numerical errors resulting from computing the derivatives can be avoided.

The simplex method works by first building a simplex, a polygon in the function space, whose vertices are the initial starting point of the variable(s), and some deviation from these variable(s). For example, if the function that is to be minimized is given by $z = z(a,b)$, then the vertices are made of

$$(a_0, b_0)$$
$$(a_0 + \delta a_0, b_0)$$
$$(a_0, b_0 + \delta b_0)$$

where the subscript '0' denotes the initial condition, and δ is the initial perturbation percentage.

The method then evaluates the function at these vertices, and finds the maximum and minimum. The method then takes the variables that gave the maximum value, and moves it in one of the predetermined ways such as contraction. The routine is repeated until the difference between the vertex that gives the highest and lowest value of the function are within a given convergence tolerance level.

Using this method for wing design, the independent variables described the geometry of the wing such as the leading edge sweep angle, and the function to be minimized was an objective function specified by the design target. More discussion on the objective function used will be given later.

AERODYNAMIC ANALYSIS METHOD

Lifting surface theory was chosen as the analysis method to determine the aerodynamic characteristics of the wing. To be more precise, the singularity-distribution method outlined in [3] was used. The singularity-distribution method is a procedure to solve the perturbation potential equation for supersonic flow. The numerical procedure outlined by Carlson and Middleton in [4] was used to solve the differential pressure coefficient distribution over the wing.

In addition to the planform, the camber distribution must be specified for the complete aerodynamic characterization of a lifting surface. PLANFOPT used Carlson's Method of component loading to determine the optimal warp for each planform iterated, which is also outlined in [4].

The inviscid drag polar was modeled using the quadratic equation shown below.

$$C_D = C_{D0} + K(C_L - C_{L0})^2$$

Here, C_D is the total inviscid drag, which consists of induced drag and wave drag due to lift, C_{D0} is the drag coefficient at a lift coefficient equal to C_{L0}, and K is the drag polar factor. The shift in the vertex of the drag polar is due to the warping of the wing, which is a complex distribution of twist and camber typical of SST's.

PLANFORM GEOMETRY DEFINITION

The variables of the function to be minimized are the parameters that describe the planform geometry of the wing. The arrow wing was chosen as the type of planform for two reasons. First, a wing with straight edges would have a lower manufacturing cost than a wing with curved edges due to simpler structural geometry and design. Second, the arrow wing is known to have a superior performance over simpler wings such as delta wings. Comparisons between the arrow and delta wing can be found in [5].

A schematic of an arrow wing is given in Figure 1. The arrow wing is defined by eight parameters: wing surface area (S), aspect ratio (AR), slenderness ratio (SL), taper ratio (λ), leading edge inner sweep angle (Λ_{LE}), trailing edge inner and outer sweep angle (Λ_{TEin}, Λ_{TEout}), and the trailing edge kink position (ε_T). The wing surface area was set constant at 9000 sq. ft. because the wing surface area is usually determined from the preliminary mission analysis. This reduced the number of variables to seven.

Given these parameters, the x and y coordinates of the six vertices can be determined. Using the surface area and the aspect ratio, the span can be found. The length of the wing is found by dividing the semi-span with the slenderness ratio, which is defined to be the ratio of the semi-span to the wing length. The geometry of the trailing edge is completely defined by the inner and outer sweep

angles and the kink location, which is normalized by the semi-span. The taper ratio will define the location where the leading edge meets the wing tip. The final point to solve is the kink location on the leading edge. This location is found so that the planform surface area will be what was specified, and from the leading edge inner sweep angle.

DESIGN CONDITION AND CONSTRAINTS/BOUNDS

The design flight condition was arbitrarily chosen as one that is typical of a SST configuration. The flight Mach number was chosen as 2.0 with a lift coefficient of 0.1. Although many of the conceptual SST studies done by various organizations call for a higher Mach number, this Mach number offers the advantage that the aerodynamic heating would be low enough that a conventional material could be used. This will also help to reduce the possible cost.

Having set the design flight condition, PLANFOPT was run for a particular case. The purpose of this first case was to verify that the results from PLANFOPT agree with the more simplified conical flow theory, and to show that additional constraints and bounds need to be specified for a realistic wing design. All seven variables were iterated in this initial trial with the objective function taken as the drag coefficient multiplied by a factor of 10^4. If during the optimization the planform became physically unrealistic, the planforms were eliminated. The three criteria for elimination were: 1) one or more of the planform edges became less than a foot in length, 2) the leading edge kink was located behind the trailing edge, and 3) the leading edge kink was located farther out spanwise than the wing tip. The simplex method does not incorporate any methods to do this, so the objective function was manually set to 10,000. This however caused problems with the optimization. It created a wall in the variable space around some initial conditions and did not allow the optimization to proceed. In order to relax this wall, the objective function was manually set to 120% of the objective function from the previous iteration. This smoothed out the objective function, and allowed the optimization to find a path to the optimum planform.

Taken from [3], the drag coefficient for a swept rectangular wing is

$$C_D = C_{de}\cos\Lambda\left(1-\sin^2\Lambda\cos^2\alpha\right)$$

Here, C_{de} is the wave drag normal to the leading edge, Λ is the leading edge sweep angle, and α is the angle of attack. Although this equation is for a rectangular wing, the general trend of the drag coefficient as the sweep changes should be the same as that with the arrow wings. The importance of this equation can immediately be seen by observing that a wing swept to the limit of 90 degrees results in a wave drag of zero. In addition, the aspect ratio ought to approach infinity, resulting in no induced drag. This would be a good way to test PLANFOPT, to see whether the planform will approach this limit.

Figure 2 shows a typical result for the above setup. The wing is extremely slender and thin, with the leading edge sweep very close to 90 degrees. The span is relatively large, which is what causes the chord to be extremely small. If both the length and the span of the wing increase, then the chord must decrease so that the wing surface area remains constant. A planform as such may mathematically be the optimum with linear theory, but there are other considerations, such as the structural design. The structural design of this wing is impossible, and in addition there are other problems such as viscous effects, placement of ailerons, etc. The aerodynamic design of a planform using PLANFOPT requires knowledge of limits to some of the parameters, which can be used to constrain and bound the planform. For PLANFOPT, these multidisciplinary considerations were based solely on engineering judgement and intuition, which will be outlined next.

Few of the variables were set as constants from multidisciplinary considerations. First, the aileron is a critical component of a wing, and will need to be placed on the inner region of the trailing edge. The structural design of this section of the wing will be simpler if there was no sweep to the inner trailing edge. The size of the ailerons will also need to be considered. It would be advantageous to reduce the chord and increase the span, rather than vice-versa, given a required aileron surface area. This would reduce complications between the placement of the actuators and other components within the wing structure. This meant that Λ_{TEin} and ε_T could be held constant. The sweep was set at 0 degrees, and the kink location was set to 0.4, or 40% of the semi-span.

Aspect ratio is another important variable that not only affects the aerodynamics of the wing, but also the structural design. Aerodynamically the drag will decrease without bound as the aspect ratio is increased, but at the same time the weight of the wing will increase, and at some point will become prohibitive. Because there is no structural model in PLANFOPT if the aspect ratio is made a variable it would increase without bound until one or more of the other constraints are violated, and if a maximum aspect ratio was set, then the resulting wing would always approach the maximum possible. Therefore,

the aspect ratio was set constant at 2.2 for now, which is again, a typical value for a SST.

Bounds were placed on the leading edge sweep, taper ratio, and the trailing edge outer sweep. A minimum on the leading edge sweep was set at 60 degrees, so that the leading edge would be inside the Mach cone at Mach 2.0, resulting in a subsonic leading edge. In reality however, the SST will have to fly transonic over land, and during transonic cruise, it will be better to have a lower sweep angle. This would however add additional complexity to the problem, and a more sophisticated model for the wing and aerodynamics would be required to evaluate the transonic performance. To keep PLANFOPT to a single point design, this was not performed.

The bounds on the trailing edge outer sweep and taper ratio were chosen by structural considerations. Too much sweep and too small of a tip chord would require a heavier structure to support the loads on the wing. The taper ratio was bound to be between 0.08 and 0.2, and a maximum for the trailing edge outer sweep was set at 35 degrees.

The final constraint set was for the kink location on the leading edge. There was really no basis for the limits, except for the fact that an arrow wing is defined by a kink on the leading edge. It was thought that if the location of the kink moved too close to the tip or the root, it would be simpler not to have the kink at all. To make sure that the kink is about the half semi-span, the location was required to be between 0.4 and 0.6, or between 40 and 60% of the semi-span.

These constraints and bounds presented were implemented using penalty functions. However, the value of the penalty had to be dependent on how much the variables deviated from their maximum or minimum values, so that the penalty function will force the optimization to find a planform that satisfies the constraints. The penalty function was formulated as the sum of each constraint normalized to a specified maximum or minimum value, added onto the objective function. For example, to force the taper ratio to be between 0.08 and 0.2, if the taper ratio became less than 0.08, then a value of $z(0.08/\lambda)^2$ was added to the objective function, and if the taper ratio became greater than 0.2, then $z(\lambda/0.2)^2$ was added. The factor z is the penalty factor used to control the strength of each constraint. The same was done for the remaining constraints, and the objective function I with the penalties is shown.

$$I = C_D x10^4 + \sum z_i \left(\frac{k_i}{k_{\max i}} \right)^2 + \sum z_i \left(\frac{k_{\min_i}}{k_i} \right)^2$$

Here, k is the value of the variables, and k_{max} and k_{min} are the maximum and minimum value for that variable. If the variable is within constraint, then the penalty is neglected. The subscript 'i' denotes that there can be as many constraints desired, and this also means that the penalty factor for each constraint can be different.

With the four components of the program (optimization routine, aerodynamic analysis, variable space, constraints/bounds) set up, it was now possible to use the code for wing design. The results will be presented in three sections; the first section will demonstrate the results from the above set up, and at the same time examine whether the final planform is dependent on the initial condition. In the second section, the constraints/bounds set on the problem will be investigated by examining how the results change as the constraints/bounds are changed. And then the final setup of the program and its results, which will be based on the results from the second part, will be presented.

DEMONSTRATION OF PLANFOPT

With any optimization problem, initial condition dependency of the converged solution is always a concern. Because the simplex method is a global optimization routine, the final planform should not depend on the initial condition, for a reasonable tolerance level. In addition, the implementation of bounds and constraints ought to guide the optimization in a common direction, regardless of the starting point.

Figures 3-6 show four initial planforms that were tested. Due to time constraints, the investigation of the initial condition dependency was limited to these cases. The initial results showed that there was some dependency on the initial condition, as shown in Figure 7. However, it was thought that these minor differences were due to numerical noise within the optimization, and could be eliminated by running the optimization a second time, with these final planforms as the initial condition, and with a smaller value for the initial deviation. It was found that repeating this routine a number of times essentially eliminated any dependency on the initial condition, as shown in Figure 8. Figures 9-12 show the histories of each variable for all four initial planforms. Again, these plot show that the final values of the variables are independent on the initial value. For the remainder of this work, it was

assumed that PLANFOPT could be used without worrying about the initial condition dependency.

The history of the optimization process for the initial planform A is shown in Figures 13 and 14. Figure 13 shows the four variables normalized to their initial values and Figure 14 shows the drag coefficient and the objective function. The planforms that were not within constraints show up as black dots above the red circles in Figure 14. The drag coefficient and the objective function decrease initially until a planform within constraints is established. From then on, only a few of the planforms violate the constraints, and the objective function decreases slowly.

Judging from this plot, it appears as if the optimization process can be divided into two steps, where the first step is not really for drag reduction, but for the search of a planform within constraints. Once that is established, a local optimization process takes place to improve the planform. Correlating the histories of the variables in Figure 13 with Figure 14 can give further insight about the optimization process. Some of the variables change very aggressively, while the others remain almost constant. Observing a different section, the passive variable will be changing quite a bit, while the one that was changing aggressively before remains about constant. This can be seen clearly with the taper ratio, slenderness ratio, and the leading edge sweep. The slenderness ratio and the leading edge sweep have an inverse relation, where if one is increasing, the other is decreasing, and vice-versa. The values for the initial and final planforms are tabulated in Tables 1 and 2.

Table 1 – Values for Initial Planforms

	Case A	Case B	Case C	Case D
SR	0.5	0.42	0.45	0.425
λ	0.15	0.12	0.35	0.5
Λ_{LE}	70.0	68.0	75.0	80.0
Λ_{TEout}	25.0	32.0	20.0	45.0
$C_D \times 10^4$	37.8	36.0	41.4	41.6

Table 2 – Values for Final Planforms

	Case A	Case B	Case C	Case D
SR	0.404	0.402	0.405	0.400
λ	0.080	0.081	0.080	0.081
Λ_{LE}	70.889	71.209	70.718	71.441
Λ_{Teout}	34.998	34.810	34.960	34.955
$C_D \times 10^4$	33.6	33.6	33.6	33.6

CHANGE CONSTRAINTS/BOUNDS

The constraints on the planform were chosen based on multidisciplinary considerations, such as the placement of the ailerons, and the feasibility of the structural design. In reality it will not be possible to design a wing based solely on aerodynamics, and compromises between the different disciplines will have to be made. With PLANFOPT it is not possible to perform these trade studies, however it is still important to understand the effects of changing the constraints.

The trailing edge kink location and the trailing edge inner sweep was held constant at an arbitrarily chosen value. These settings were examined by running cases with the kink location set at 0.2, 0.3, 0.5 and 0.6. Finally the location was made a variable.

Figure 15 compares some of the final planforms with different settings for the kink location, and Figure 16 shows the final planform for the variable kink location case. There were a few obvious trends in the solution, one being that the closer the kink was to the wing root, the lower the drag coefficient. For the case where the kink location was made a variable, the kink moved all the way to the root, until the inner trailing edge reached the minimum one foot. Figure 17 shows the trend in the drag coefficient as the kink location was changed.

A similar study was done on the effect of changing the sweep of the inner trailing edge. The sweep was set at -20, -10, 10, and 20 degrees, and then allowed to change. Some of the results are shown in Figures 18 and 19. As the sweep is increased, there is a decrease in the drag coefficient. This is shown graphically in Figure 20. When the inner trailing edge sweep was a variable, the final planform had an inner trailing edge sweep of 47 degrees. At first there seemed to be no significance to this particular value, but examining the rest of the variables, it was found that the taper ratio and the trailing edge outer sweep had reached their minimum and maximum values. This implies that if there were no bounds on the taper ratio and outer trailing edge sweep, the inner trailing edge sweep would approach 90 degrees.

These results agree with what was presented earlier in Figure 2, where the aerodynamically optimal wing had the kink location near the wing root and an extremely large trailing edge sweep. These trends can be seen in Figures 16 and 19, and if it were not for the other constraints on the taper ratio, leading edge kink location, etc., the wing would approach the one in Figure 2.

Another result that was shown in these two studies, although not obvious from looking at the

planforms, was that the taper ratio always approached 0.08, and the trailing edge outer sweep always approached 35 degrees. This was significant, because these were the minimum and maximum values set in the constraints. Like the kink location approaching 0.0, the taper ratio wanted to go to zero, and the trailing edge outer sweep wanted to go to 90 degrees. Because of this, the resulting wing should have the smallest allowed taper ratio and the largest allowed trailing edge outer sweep, regardless of the value of the bound. This was investigated by running four cases with different settings for the maximum and minimum for taper ratio and trailing edge outer sweep. The minimum taper ratio was changed to 0.06 and 0.1, and the maximum trailing edge outer sweep was changed to 30 and 40 degrees.

Some of the results are shown in Figure 21. The predicted trend did happen, and the taper ratio and trailing edge outer sweep approached their limits. This result was actually very powerful because it meant that the taper ratio and the trailing edge outer sweep should not be iterated, because they will go to their limits chosen by the user. Instead, the taper ratio and the trailing edge outer sweep should simply be chosen and kept constant, which will simplify the problem and shorten the turnaround time. The results from these cases are tabulated below in Table 3.

Table 3 – Results of Cases of Different Limits on Trailing Edge Outer Sweep and Taper Ratio

	$\lambda_{min} = 0.06$	$\lambda_{min} = 0.1$
$TE_{max} = 30$ deg.	$C_D \times 10^4 = 34.1$ $\Lambda_{LE} = 69.9$ deg. SR = 0.42	$C_D \times 10^4 = 34.7$ $\Lambda_{LE} = 69.3$ deg. SR = 0.43
$TE_{max} = 40$ deg.	$C_D \times 10^4 = 32.6$ $\Lambda_{LE} = 72.9$ deg. SR = 0.37	$C_D \times 10^4 = 33.1$ $\Lambda_{LE} = 71.2$ deg. SR = 0.39

These results agree with what was shown in Figure 2. The cases with the larger trailing edge sweep and the smaller taper ratio have the lower drag. Also, there is a correlation between the drag and the slenderness ratio, or the length of the wing, because the aspect ratios for all four cases are the same. The longer wing also has a larger leading edge sweep, implying a lower wave drag due to lift. Because the induced drag is dependent almost solely on the aspect ratio, the differences in the drags are due to the leading edge of the wing. This suggests that the reason why a small taper ratio and a larger trailing edge sweep is desired is because if the aspect ratio is the same, then the leading edge sweep will be allowed to be larger.

The last family of cases ran were for different values of the aspect ratio. For these cases, the result from the previous study was used, and the taper ratio and the trailing edge outer sweep were also set a constant, along with the trailing edge kink location and the trailing edge inner sweep. The taper ratio was 0.08 and the trailing edge outer sweep was 35 degrees. The aspect ratio was set from 1.4 to 2.8.

Some of the results are plotted in Figure 22. The planforms of the smaller aspect ratios are much longer because of the constraint on the surface area. Because the taper ratio and the trailing edge outer sweep are now held constant, the only parameters iterated are the leading edge sweep and the slenderness ratio. It was desired to make the aspect ratio also a variable, because the aspect ratio is a parameter that greatly influences the performance of a wing. This was however unfavorable, because it was already shown earlier that the aspect ratio wanted to be as large as it was allowed to be. Comparing the drag coefficients of the wings from the last study however provided new information, and was used for the final setup of PLANFOPT.

FINAL SETUP OF PLANFOPT

The drag coefficients as a function of the aspect ratio are plotted in Figure 23. As the aspect ratio increases, the overall drag goes down, because the induced drag is decreasing. However, at some point, aspect ratio of 2.4 for this case, there is a minimum point in the plot. If the cause of this parabolic behavior in the drag can be determined, the aspect ratio can also be made a variable, because it will no longer approach infinity, there is an optimum aspect ratio.

From elementary supersonic aerodynamics, the inviscid drag on a wing is composed of the induced drag and the wave drag due to lift. At first after seeing the result in Figure 2, it was believed that the two drags are independent of each other, in the sense that the code will change the wing in such a way that both will decrease or increase. This was what happened with the initial case run, but after the implementation of the constraints and bounds, the problem was set up in such a way that the induced drag and the wave drag could have an inverse relation with each other.

PLANFOPT, in general, changes the planform so that the span and the length increase and that is why an unconstrained optimization will result in a wing such as that in Figure 2. From Figure 22, as the aspect ratio increases the length decreases, and consequently the leading edge sweep must decrease, to maintain the constant surface area. If the aspect

ratio is too large, the planform will become too short with not enough sweep, increasing the wave drag, and if the wing is swept too much causing the planform to be long, then the aspect ratio will not be large enough and the induced drag will increase. The planform of lowest drag will be one where the aspect ratio and the leading edge sweep will be such that the induced drag and the wave drag due to lift are balanced, but not necessarily equal. Finding the planform parameters to achieve this, for a given flight condition and multidisciplinary constraints will therefore be the final setup of PLANFOPT. A description of the final structure of PLANFOPT and how it will fit into the overall design process of an aircraft will be briefly given next.

During the preliminary design stage of an aerospace system, the system parameters are determined. For transport aircraft aerodynamics, these are usually the cruise velocity and altitude, design lift coefficient, and wing surface area. The altitude can be combined with velocity to give flight Mach number. These three parameters that come from the preliminary design will be one of the two kinds of inputs to PLANFOPT, the flight condition. The second kind of inputs to PLANFOPT will be the constraints and bounds, which will be supplied by the designers of the other disciplines. These will be the trailing edge sweep, kink location, and taper ratio. PLANFOPT will then take these inputs, and find the aspect ratio, leading edge sweep, and slenderness ratio that will give a planform with the lowest inviscid drag. Higher level methods such as CFD design methods can then be used to solve for the detailed aerodynamics of the wing.

A sample study of changing the flight condition was done by varying the design Mach number. It was assumed that the weight of the aircraft and the altitude are constant, so that the product of Mach number squared and lift coefficient will be a constant. The Mach numbers were set to 1.6, 2.0, 2.6, and 3.0. Some of the results are shown in Figure 24. As the Mach number is increased the wing becomes more slender and arrow-like. As the Mach number increases, a larger leading edge sweep angle is needed, and because of the constraints, a larger length is needed. The surface area is a constant, so the aspect ratio must decrease along with the slenderness ratio. The final values of the three variables are plotted against the design Mach numbers in Figures 25-27. The plots show exactly what was stated above. And finally the drag coefficients are plotted in Figure 28, and the L/D is plotted in Figure 29. As the Mach number is increased, the lift coefficient decreases, and so does the drag coefficient. However, because the wave drag decreases faster, the L/D increases with Mach number.

CONCLUSION

A preliminary design tool for a supersonic wing planform has been developed. The parameters that strongly influence the aerodynamic performance of the wing were made primary variables. These consisted of the aspect ratio, leading edge sweep, and the slenderness ratio. The parameters that were made constants, the trailing edge sweep, trailing edge kink location, and taper ratio, can be classified as secondary variables, because they do not directly influence the aerodynamic performance, but bound the primary variables. This classification agrees with conical theory, in that for a swept rectangular wing, the leading edge sweep and the aspect ratio are what influence the inviscid drag. Iterating only the primary variables helped to reduce the independent variables, which is always desirable because of the shorter turnaround time, especially with advanced optimization routines and aerodynamic models in the future

The fact that the variables can be grouped into two categories shows that even a preliminary planform design is a multidisciplinary problem. If the planform is designed through aerodynamic consideration only, then the resulting planform will have the maximum aspect ratio and leading edge sweep allowed through the geometry definition. This will result in a physically unrealistic planform, which may have a very low drag, but not possible to manufacture.

Looking at the results from the final setup, the trends in the designed wings agree with the simpler theories and with actual aircraft in existence. A high Mach number results in a highly swept arrow wing, and as the Mach number is reduced, the wing becomes less swept with a larger aspect ratio. This is so that the induced drag and the wave drag due to lift are balanced, but not necessarily equal. Finally, it was shown that the L/D increases with design Mach number, if the weight of the aircraft, wing surface area, and the flight altitude are kept constant.

REFERENCES

[1] Y. Shimbo, K. Yoshida. warpplanf, warpdgn. National Aerospace Laboratory FORTRAN codes.

[2] B. Flannery, W. Press, S. Teukolsky, W. Vetterling. Numerical Recipes in FORTRAN 2nd Ed. Cambridge University Press Copyright 1992.

[3] J. J. Bertin and M. L. Smith. Aerodynamics for Engineers. Prentice Hall Copyright 1989.

[4] D. Kuchemann. The Aerodynamic Design of Aircraft. Pergamon Press Copyright 1978

[5] B.R. Wright, F. Bruckman, N.A. Rodovcich. Arrow Wings for Supersonic Cruise Aircraft. Journal of Aircraft Vol. 15, No. 12, December 1978

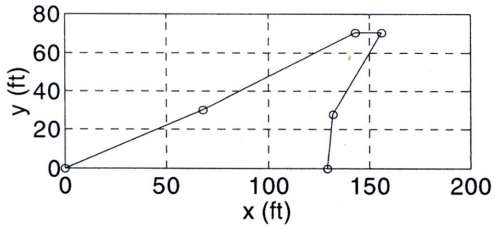

Figure 1 – Sample Arrow Wing

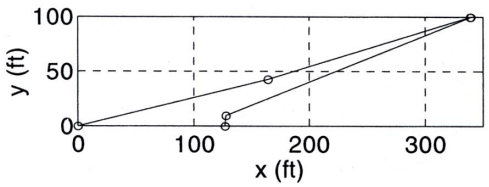

Figure 2 – Optimization with No Constraints

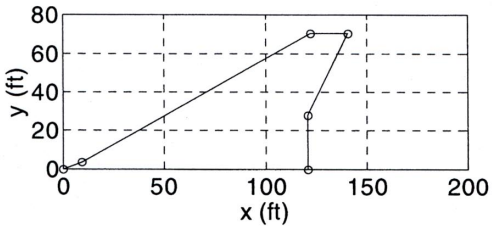

Figure 3 – Initial Condition A

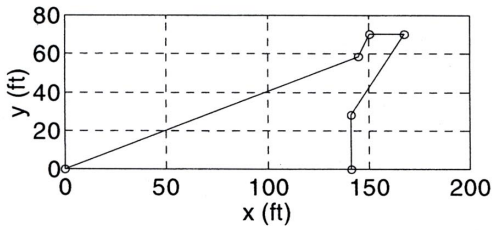

Figure 4 – Initial Condition B

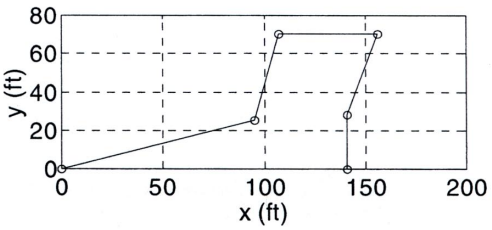

Figure 5 – Initial Condition C

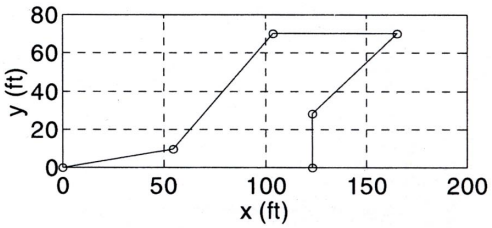

Figure 6 – Initial Condition D

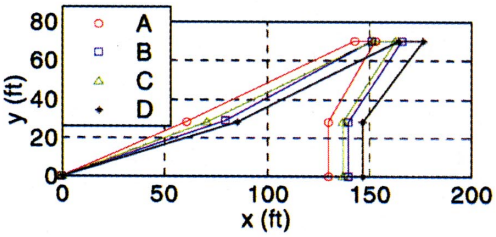

Figure 7 – Final Planforms After First Run

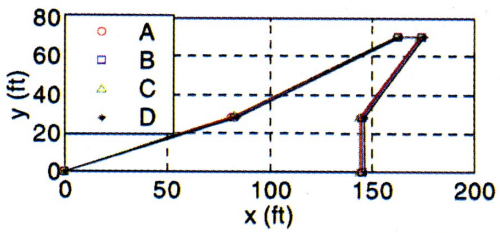

Figure 8 – Final Planforms

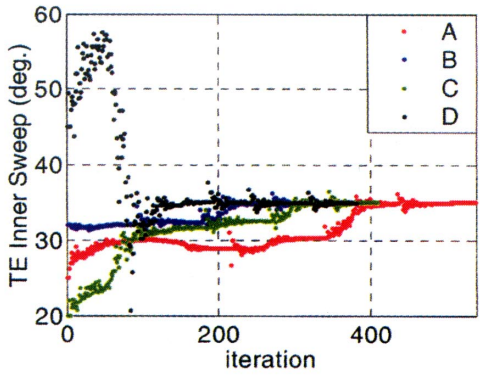

Figure 9 – Histories of Trailing Edge Outer Sweep

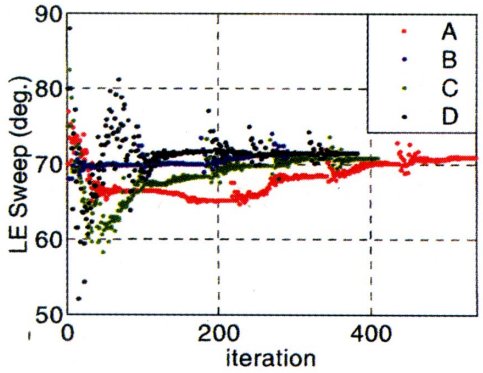

Figure 10 – Histories of Leading Edge Sweep

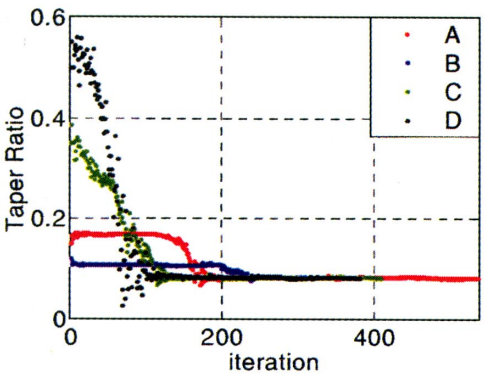

Figure 11 – Histories of Taper Ratio

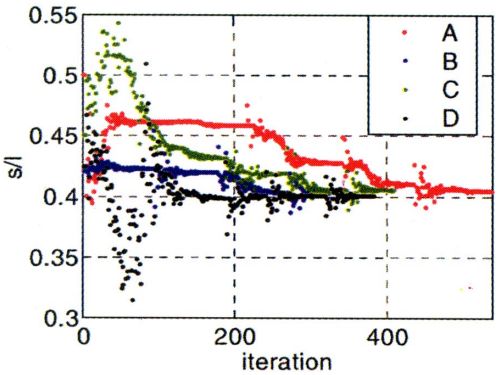

Figure 12 – Histories of Slenderness Ratio

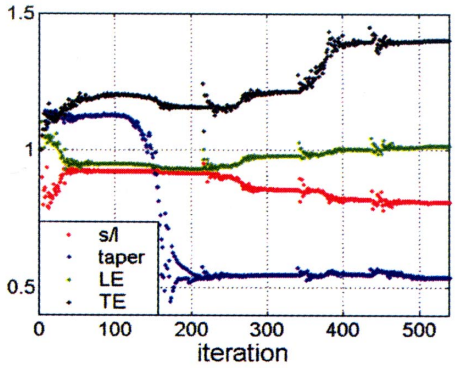

Figure 13 – Histories of Variables for Case A

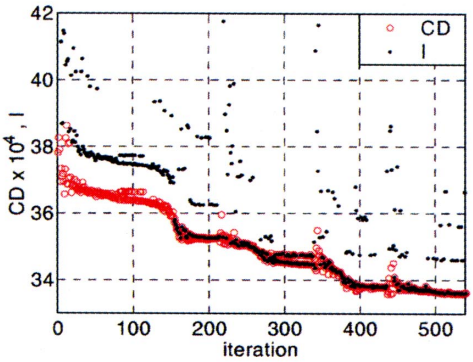

Figure 14 – History of Drag and Obj. Func. For Case A

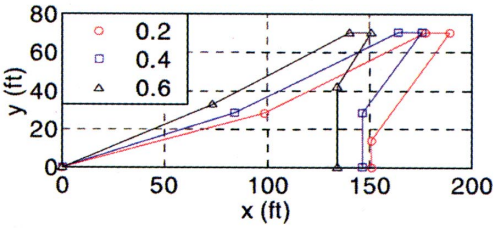

Figure 15 – Various Settings for the Trailing Edge Kink Location

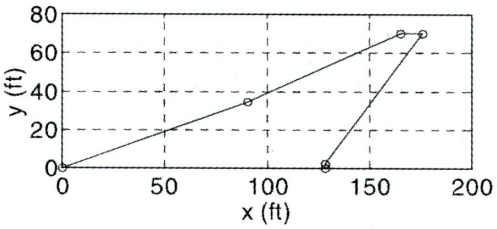

Figure 16 – Trailing Edge Kink Location is a Variable

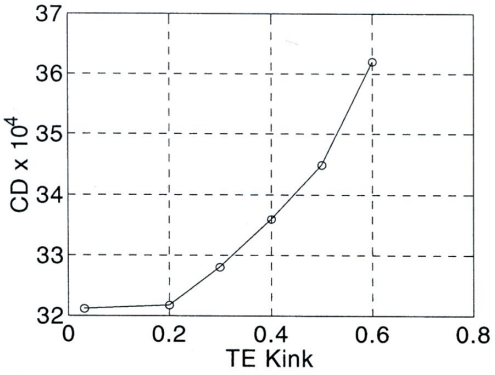

Figure 17 – C_D for Varying Trailing Edge Kink Location

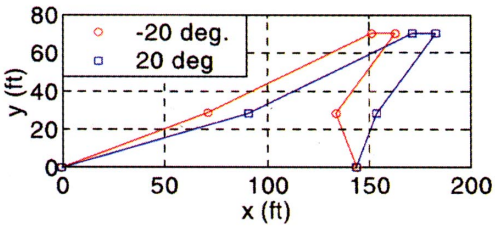

Figure 18 – Various Settings for the Trailing Edge Inner Sweep Angle

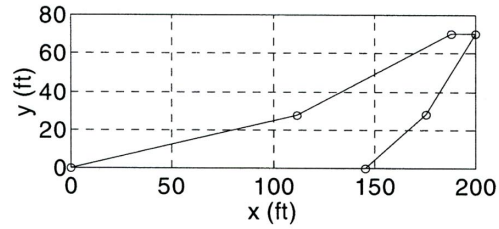

Figure 19 – Trailing Edge Inner Sweep Angle is a Variable

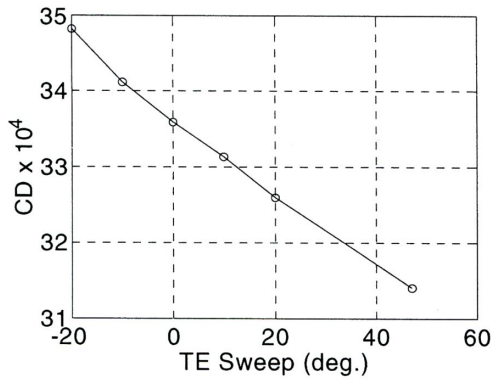

Figure 20 – C_D for Varying Trailing Edge Inner Sweep Angle

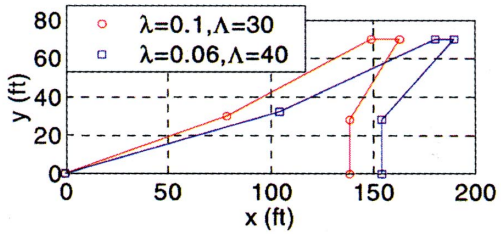

Figure 21 – Samples of Changing Maximum Trailing Edge Outer Sweep Angle and Minimum Taper Ratio

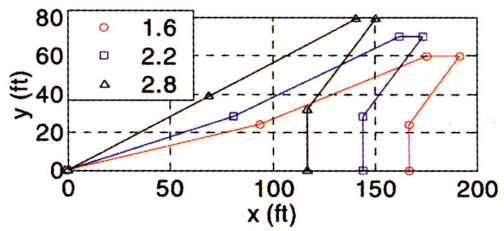

Figure 22 – Various Settings for the Aspect Ratio

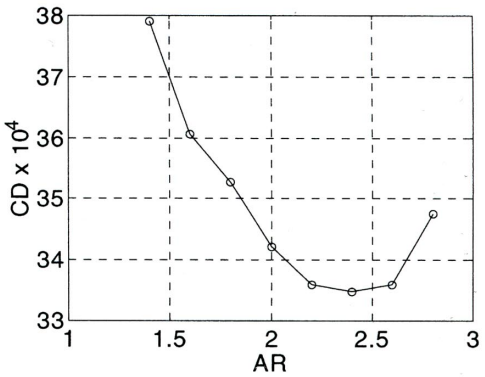

Figure 23 – C_D for Varying Aspect Ratio

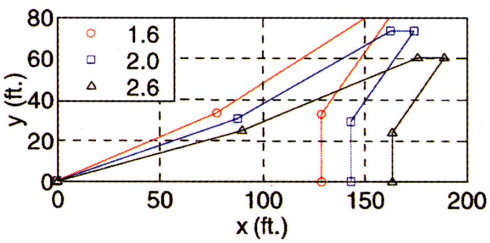

Figure 24 – Various Settings of Flight Mach Number and Corresponding C_L

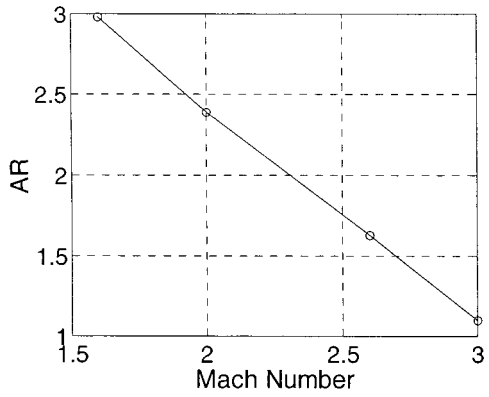

Figure 25 – Aspect Ratio for Varying Mach Number

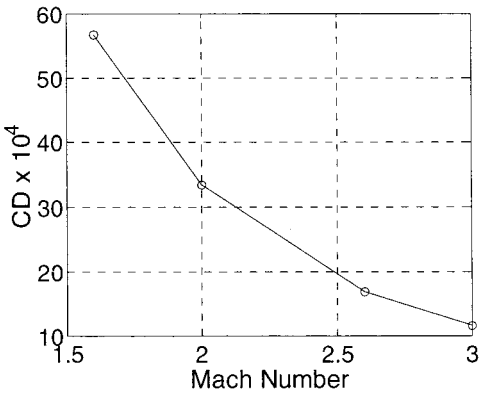

Figure 28 – C_D for Varying Mach Number

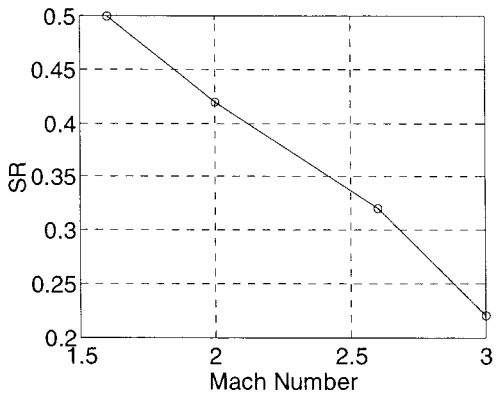

Figure 26 – Slenderness Ratio

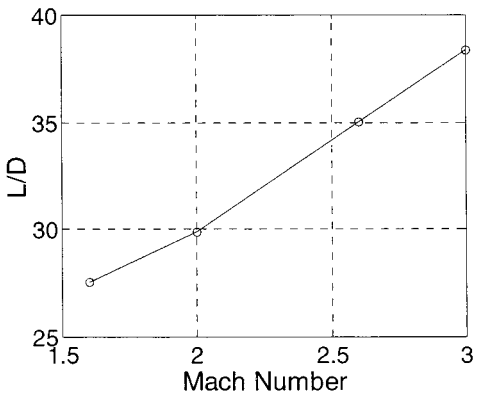

Figure 29 – L/D for Varying Mach Number

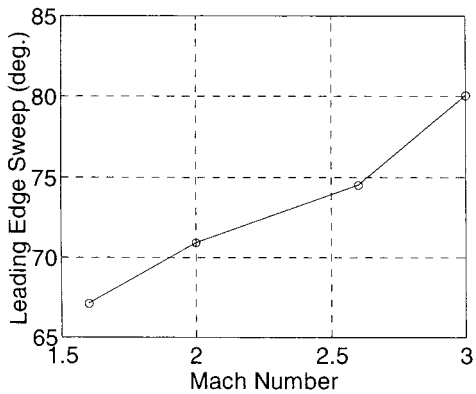

Figure 27 – Leading Edge Sweep Angle